Age-dependent increase in angiopoietin-like protein 2 accelerates skeletal muscle loss in mice

Received for publication, September 3, 2017, and in revised form, November 20, 2017 Published, Papers in Press, November 30, 2017, DOI 10.1074/jbc.M117.814996

Jiabin Zhao[‡1], Zhe Tian[‡1,2], Tsuyoshi Kadomatsu[‡], Peiyu Xie[‡], Keishi Miyata[‡§], Taichi Sugizaki[‡], Motoyoshi Endo[‡], Shunshun Zhu[‡], Haoqiu Fan[‡], Haruki Horiguchi[‡], Jun Morinaga[‡], Kazutoyo Terada[‡], Tatsuya Yoshizawa[¶], Kazuya Yamagata[¶], and Yuichi Oike[‡3]

From the Departments of [‡]Molecular Genetics, [§]Immunology, Allergy, and Vascular Biology, and [¶]Medical Biochemistry, Graduate School of Medical Sciences, Kumamoto University, Kumamoto 860-8556, Japan

Edited by Velia M. Fowler

Skeletal muscle atrophy, or sarcopenia, is commonly observed in older individuals and in those with chronic disease and is associated with decreased quality of life. There is recent medical and broad concern that sarcopenia is rapidly increasing worldwide as populations age. At present, strength training is the only effective intervention for preventing sarcopenia development, but it is not known how this exercise regimen counteracts this condition. Here, we report that expression of the inflammatory mediator angiopoietin-like protein 2 (ANGPTL2) increases in skeletal muscle of aging mice. Moreover, in addition to exhibiting increased inflammation and accumulation of reactive oxygen species (ROS), denervated atrophic skeletal muscles in a mouse model of denervation-induced muscle atrophy had increased ANGPTL2 expression. Interestingly, mice with a skeletal myocyte–specific *Angptl2* knockout had attenuated inflammation and ROS accumulation in denervated skeletal muscle, accompanied by increased satellite cell activity and inhibition of muscular atrophy compared with mice harboring wildtype *Angptl2*. Moreover, consistent with these phenotypes, wildtype mice undergoing exercise training displayed decreased ANGPTL2 expression in skeletal muscle. In conclusion, ANGPTL2 up-regulation in skeletal myocytes accelerates muscle atrophy, and exercise-induced attenuation of ANGPTL2 expression in those tissues may partially explain how exercise training prevents sarcopenia.

This work was supported by Scientific Research Fund of the Ministry of Education, Culture, Sports, Science and Technology (MEXT) of Japan Grant 17H05652 (to Y. O.), Core Research for Evolutional Science and Technology (CREST) Programme of the Japan Science and Technology Agency (JST) Grant 13417915 (to Y. O.), the CREST Programme of the Japan Agency for Medical Research and Development (AMED) Grant 17gm0610007h0005 (to Y. O.), and by the Project for Elucidating and Controlling Mechanisms of Aging and Longevity from AMED. The authors declare that they have no conflicts of interest with the contents of this article.
This article contains Figs. S1–S4 and Table S1.

[1] Both authors contributed equally to this work.
[2] To whom correspondence may be addressed: Dept. of Molecular Genetics, Graduate School of Medical Sciences, Kumamoto University, 1-1-1 Honjo, Chuo-ku, Kumamoto 860-8556, Japan. Tel.: 81-96-373-5142; Fax: 81-96-373-5145; E-mail: zhetian0118@gmail.com.
[3] To whom correspondence may be addressed: Dept. of Molecular Genetics, Graduate School of Medical Sciences, Kumamoto University, 1-1-1 Honjo, Chuo-ku, Kumamoto 860-8556, Japan. Tel.: 81-96-373-5142; Fax: 81-96-373-5145; E-mail: oike@gpo.kumamoto-u.ac.jp.

Sarcopenia is defined as age-related loss of skeletal muscle mass and strength, a condition that worsens quality of life (1). Sarcopenia is now a medical and social concern because the aging population is increasing worldwide. Sarcopenia also develops in patients with chronic disease, such as diabetes, cardiovascular disease, and cancer, and these pathologies accelerate clinical mortality (2). Therefore, clarification of molecular mechanisms underlying sarcopenia development is important to devise effective therapeutic and/or preventive approaches to treat this condition.

Several lines of evidence support the idea that in skeletal muscle chronic inflammation and reactive oxygen species (ROS)[4] accumulation due to redox imbalance contribute to sarcopenia development (3–8). Chronic inflammation in aging skeletal muscle is positively correlated with sarcopenia development in humans and mice (3, 4). The pro-inflammatory cytokines interleukin-6 (IL-6) and interleukin-1β (IL-1β) both decrease skeletal muscle mass by causing inflammation and subsequently facilitating muscle proteolysis, ROS accumulation, and growth hormone resistance (9–11). Moreover, excess ROS accumulation causes oxidative damage to skeletal muscles, resulting in loss of myofibers (5–8). Both inflammation and ROS accumulation inactivate "satellite cells," the precursors of skeletal muscle cells (12, 13), thereby accelerating sarcopenia development (14). Currently, strength training exercise, which increases the volume of skeletal muscle myofibers, is the only effective way to prevent sarcopenia development. Recent reports suggest that exercise reduces inflammation (15) and ameliorates ROS accumulation by increasing antioxidant activity (16) and also enhances satellite cell activation (17) in animal models of aging. However, molecular mechanisms underlying these activities remain unclear.

Previous studies reveal that expression and secretion of angiopoietin-like 2 (ANGPTL2) significantly increase in cells stressed by pathophysiological stimuli, such as hypoxia and pressure overload (18, 19). ANGPTL2 expression also increases in cells undergoing senescence (20, 21), suggesting that

[4] The abbreviations used are: ROS, reactive oxygen species; WGA, wheat germ agglutinin; CBB, Coomassie Brilliant Blue; ANOVA, analysis of variance; SMC, skeletal myocyte; 4-HNE, 4-hydroxynonenal; SASP, senescence-associated secretory phenotype; AICAR, 5-aminoimidazole-4-carboxamide-1-β-D-ribofuranoside; PPAR, peroxisome proliferator-activated receptor; CM-H2DCFDA, 5-(and -6)-chloromethyl-2′,7′-dichlorodihydrofluorescein diacetate acetyl ester.

ANGPTL2 is a senescence-associated secretory phenotype (SASP) factor. Moreover, excess ANGPTL2 signaling is pro-inflammatory in pathological states and contributes to development of aging-associated diseases such as obesity, diabetes, atherosclerotic disease, chronic kidney disease, and some cancers (22, 23).

Although ANGPTL2 hyperactivation is associated with age-related diseases, ANGPTL2 function in sarcopenia development remains unknown. Here, we investigated the roles of ANGPTL2 in sarcopenia development using aging mice and denervation-induced muscle atrophy mouse model. We report that ANGPTL2 expression increases in skeletal myocytes of aging mice and that running exercise decreases that expression, suggesting that excess ANGPTL2 signaling in aged skeletal muscular myofibers accelerates sarcopenia development. Moreover, ANGPTL2 deficiency in skeletal myocytes attenuated loss of skeletal muscle by reducing muscular inflammation and ROS accumulation and increasing satellite cell activity. To the best of our knowledge, this is the first report showing that ANGPTL2 signaling may accelerate sarcopenia pathologies.

Results

ANGPTL2 expression increases in skeletal myocytes with age

Because ANGPTL2 expression and its circulating levels are positively correlated with aging (19, 23, 24), we asked whether ANGPTL2 expression increases in aging skeletal muscles. To do so, we first evaluated age-related changes in skeletal muscles of adult (8-month-old) compared with aging (18-month-old) mice. We observed significantly increased expression of pro-inflammatory and cellular senescence genes in skeletal muscle of aging relative to adult mice (Fig. 1*a*). Skeletal muscle mass of aging mice was significantly decreased compared with that seen in adult mice (Fig. 1*b*). In animal tissues, 4-hydroxynonenal (4-HNE) is a lipid peroxidation product whose formation is closely related to oxidative stress (25). Because of its electrophilic nature, 4-HNE reacts with nucleophilic amino acid residues to form 4-HNE-adducted proteins, which serves as a marker of oxidative stress. We also confirmed increased 4-HNE-adducted protein levels and decreased catalase expression in skeletal muscle of aging relative to adult mice; however, we observed no change in expression of superoxide dismutases (*Sods*) or glutathione peroxidase 1 (*Gpx1*) (Fig. 1, *c* and *d*). Moreover, expression of genes associated with satellite cell activation, such as *Cd34*, *Pax3*, and *Pax7*, in skeletal muscles was significantly decreased in aging relative to adult mice (Fig. 1, *e* and *g*, and Fig. S1, *a* and *b*).

We next evaluated ANGPTL2 expression in aging and adult mice. *Angptl2* mRNA and protein levels significantly increased in skeletal muscle tissues of aging relative to adult mice (Fig. 1, *f* and *g*). Skeletal muscle tissue is composed not only skeletal myocytes but of various stromal cells, such as endothelial cells, macrophages, and infiltrated blood cells. Thus, to determine which cell type in skeletal muscle predominantly expresses ANGPTL2, we prepared both skeletal myocyte (SMC)- and stromal cell-enriched fractions from skeletal muscle of adult and aging mice (Fig. S2). In adult mice, ANGPTL2 protein levels were comparable in both fractions, but in aging mice, ANGPTL2 protein expression was markedly increased in the SMC fraction relative to the stromal cell fraction (Fig. 1*h*). These results suggest that ANGPTL2 is predominantly increased in skeletal myocytes of aging mice.

ANGPTL2 suppression in skeletal myocytes decreases inflammation and ROS levels and improves cellular senescence phenotypes

To determine the relationship between *Angptl2* expression in skeletal myocytes and age-related changes in skeletal muscle, we generated skeletal myocyte–specific *Angptl2* knockout (*Angptl2*$^{Flox/Flox}$;*MCK-Cre*) mice. We first confirmed that both *Angptl2* mRNA and protein expression were decreased by half in *Angptl2*$^{Flox/Flox}$;*MCK-Cre versus Angptl2*$^{Flox/Flox}$ mice (Fig. 2*a*) and that expression was specifically decreased in skeletal myocytes (Fig. 2*b*). Skeletal muscle masses were comparable between *Angptl2*$^{Flox/Flox}$;*MCK-Cre* and *Angptl2*$^{Flox/Flox}$ mice (Fig. 4*a*), suggesting that ANGPTL2 deficiency in skeletal myocytes does not alter myogenesis or skeletal muscle homeostasis.

Moreover, expression of pro-inflammatory and cellular senescence genes in skeletal muscle significantly decreased in *Angptl2*$^{Flox/Flox}$;*MCK-Cre* relative to *Angptl2*$^{Flox/Flox}$ mice (Fig. 2*c*). In addition, although we observed slightly decreased ROS levels in some low-molecular-weight proteins, there was no significant difference in global ROS levels in young skeletal muscle of either genotype (Fig. 2*d*). However, catalase activity in skeletal muscle of *Angptl2*$^{Flox/Flox}$;*MCK-Cre* mice was significantly higher than that seen in *Angptl2*$^{Flox/Flox}$ mice (Fig. 2*e*).

To further assess the effect of ANGPTL2 suppression on myocytes, we conducted loss-of-function studies by transfecting differentiated mouse C2C12 myoblasts with Angptl2 siRNA or control siRNA. ANGPTL2 protein levels were significantly decreased in Angptl2-knockdown cells and in their culture medium compared with control cells (Fig. 2*f* and Fig. S3*a*). Expression levels of *p21*, *p57*, and *Il-6* and senescence-associated β-gal activity were all significantly decreased in Angptl2 knockdown relative to control C2C12 cells (Fig. 2, *g* and *h*). Moreover, intracellular ROS levels in Angptl2 knockdown cells were significantly lower than those in control cells, whereas catalase expression and activity were significantly increased in knockdown relative to control cells (Fig. 2, *i* and *j*). These results suggest that ANGPTL2 suppression in skeletal myocytes enhances ROS clearance capacity by up-regulating catalase and decreasing inflammation and cellular senescence phenotypes.

ANGPTL2 deficiency in myocytes increases skeletal muscle satellite cell activity

Because inflammation and ROS antagonize development of skeletal muscle satellite cells (26), we evaluated satellite cell activity in skeletal muscle of *Angptl2*$^{Flox/Flox}$;*MCK-Cre* and *Angptl2*$^{Flox/Flox}$ mice. Expression of genes associated with satellite cell activation in *Angptl2*$^{Flox/Flox}$;*MCK-Cre* mice was significantly increased compared with that seen in *Angptl2*$^{Flox/Flox}$ mice (Fig. 3*a*). Moreover, immunofluorescence staining revealed that the number of quiescent satellite cells (marked by $CD34^+/PAX7^+$ expression) did not change; however, the number of activated satellite cells (as marked by $CD34^-/PAX7^+$ expression) increased in skeletal muscle of *Angptl2*$^{Flox/Flox}$;

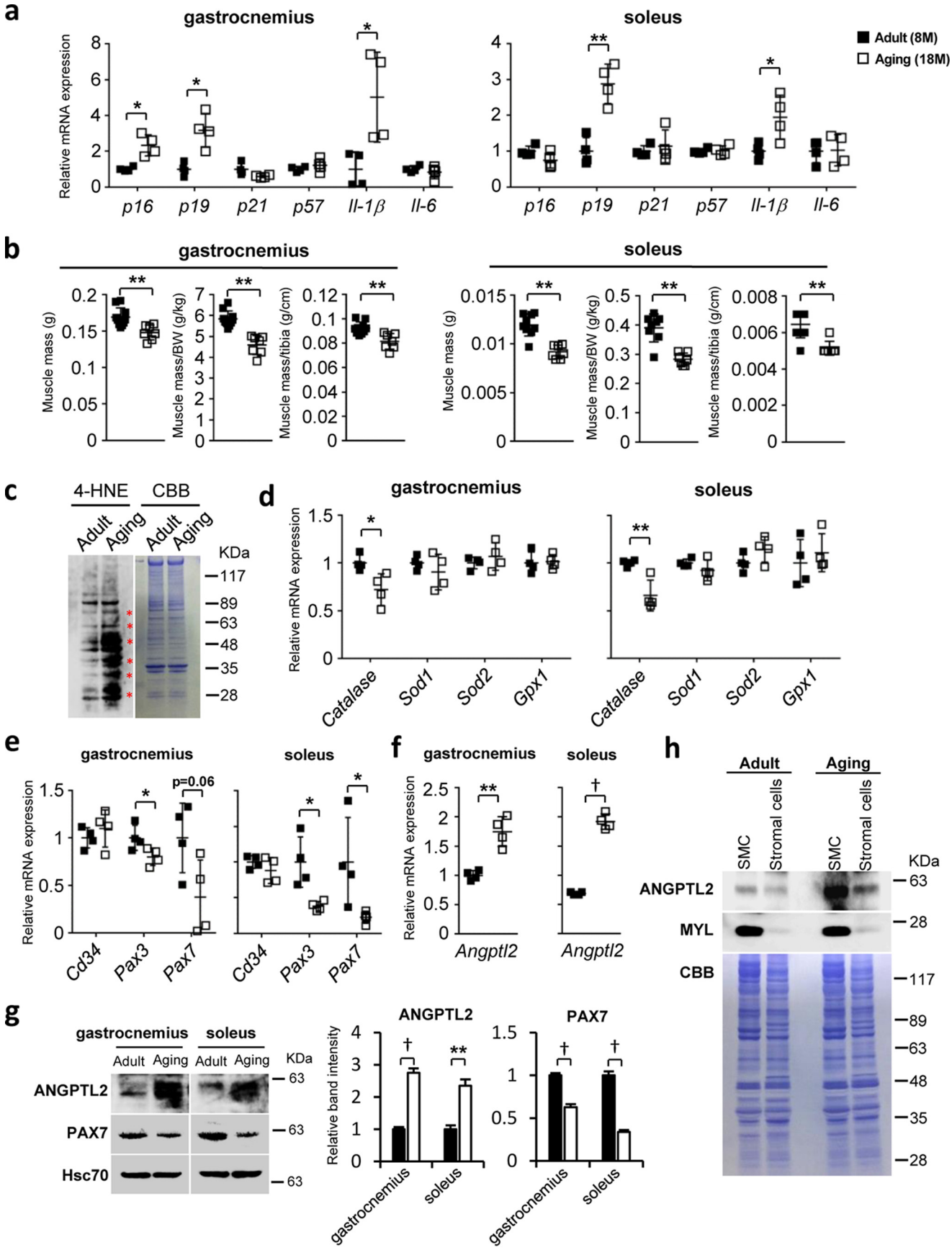
a
gastrocnemius
soleus
Adult (8M)
Aging (18M)
Relative mRNA expression
p16
p19
p21
p57
Il-1β
Il-6
b
gastrocnemius
soleus
Muscle mass (g)
Muscle mass/BW (g/kg)
Muscle mass/tibia (g/cm)
c
4-HNE
CBB
Adult
Aging
KDa
117
89
63
48
35
28
d
gastrocnemius
soleus
Relative mRNA expression
Catalase
Sod1
Sod2
Gpx1
e
gastrocnemius
soleus
Relative mRNA expression
p=0.06
Cd34
Pax3
Pax7
f
gastrocnemius
soleus
Relative mRNA expression
Angptl2
g
gastrocnemius
soleus
Adult
Aging
KDa
ANGPTL2
PAX7
Hsc70
63
Relative band intensity
h
Adult
Aging
SMC
Stromal cells
KDa
ANGPTL2
MYL
CBB
63
28
117
89
63
48
35
28

MCK-Cre relative to *Angptl2*$^{Flox/Flox}$ mice (Fig. 3*b* and Fig. S3*c*). Immunoblotting analysis also revealed relatively increased PAX7 protein levels in skeletal muscle of *Angptl2*$^{Flox/Flox}$*;MCK-Cre* mice (Fig. 3*c*). Overall, these results suggest that ANGPTL2 suppression in skeletal myocytes promotes satellite cell activation without any impairing of their self-renewal.

ANGPTL2 deficiency in myocytes prevents skeletal muscle atrophy

Because aging-associated inflammation, ROS accumulation, and satellite cell inactivation all reportedly contribute to sarcopenia (7, 27, 28), we asked whether ANGPTL2 deficiency in skeletal myocytes would protect skeletal muscles from atrophy. Given that spinal motor neuron loss and reduced numbers of motor units characterize aging and directly induce sarcopenia (29), we established a denervation-induced muscle atrophy mouse model to mimic sarcopenia. As anticipated, we observed a significant decrease in skeletal muscle mass relative to wildtype by 7 days after denervation (Fig. S4).

We also observed relatively increased ANGPTL2 protein expression in skeletal muscle post-denervation (Fig. 4*b*). To assess the pathophysiological significance of this increase, we performed denervation in *Angptl2*$^{Flox/Flox}$*;MCK-Cre* mice. By 14 days after denervation, the reduction in skeletal muscle mass seen in wildtype *Angptl2* mice was significantly suppressed in *Angptl2*$^{Flox/Flox}$*;MCK-Cre* mice (Fig. 4, *c* and *d*). Decreased cellular volume seen on a wildtype *Angptl2* background was also significantly suppressed in *Angptl2*$^{Flox/Flox}$*;MCK-Cre* mice (Fig. 4, *e* and *f*), suggesting overall that ANGPTL2 deficiency in skeletal myocytes prevents development of muscle atrophy.

Angptl2$^{Flox/Flox}$*;MCK-Cre* mice also showed decreased expression of pro-inflammatory genes in denervated skeletal muscle compared with *Angptl2*$^{Flox/Flox}$ mice (Fig. 5*a*). By 14 days after denervation, ROS accumulation and decreased catalase expression seen in denervated skeletal muscle of mice harboring wildtype *Angptl2* were significantly suppressed in *Angptl2*$^{Flox/Flox}$*;MCK-Cre* mice (Fig. 5, *b* and *c*). Expression levels of genes associated with satellite cell activation and PAX7 protein in skeletal muscle were also significantly increased in *Angptl2*$^{Flox/Flox}$*;MCK-Cre* mice compared with mice harboring wildtype *Angptl2* (Fig. 5, *d* and *e*). These results suggest that ANGPTL2 deficiency in skeletal myocytes blocks muscle atrophy by activating satellite cells and decreasing inflammation and ROS accumulation.

Exercise training suppresses ANGPTL2 expression in skeletal muscle

Because exercise training reportedly prevents sarcopenia development (30), we asked whether exercise altered *Angptl2* expression in skeletal muscle. To do so, we exposed wildtype mice to exercise training involving running on a treadmill (see "Experimental procedures"). We first confirmed that after exercise training, expression of pro-inflammatory or cellular senescence genes in skeletal muscles significantly decreased and that of genes associated with satellite cell activation significantly increased (Fig. 6, *a* and *b*), as reported previously (15–17). Moreover, expression of *Angptl2* mRNA and protein in skeletal muscle was significantly decreased after exercise training (Fig. 6, *c* and *d*).

To further evaluate the effect of exercise training on *Angptl2* expression in skeletal myocytes, we used two cellular exercise models in which differentiated C2C12 cells are either subjected to mechanical stretch or treated with AICAR (AMP-activated kinase activator) (31, 32), both of which lead to cellular changes associated with exercise training. *Angptl2* expression levels in differentiated C2C12 cells significantly decreased after mechanical stretch (Fig. 6*e*), whereas AICAR treatment of C2C12 cells also significantly decreased expression of *Angptl2* mRNA and protein (Fig. 6*f*).

Discussion

This study reveals that ANGPTL2 expression in skeletal myocytes increases with age and in a denervation-induced muscle atrophy mouse model. Interestingly, *Angptl2*-deficient mice in the atrophy model showed relatively decreased inflammation and ROS accumulation and increased satellite cell activity. In sarcopenia development, both inflammation and excess ROS accumulation damage skeletal myocytes and inactivate satellite cells, accelerating muscle mass loss (14). Taken together, these findings suggest that ANGPTL2 contributes to sarcopenia development by accelerating inflammation and ROS accumulation in skeletal muscle and subsequently inactivating satellite cells.

Large amounts of ROS released from senescent skeletal myocytes may enhance oxidative damage to skeletal muscle (33). Excessive ROS accumulation with age is reportedly due to decreased activity and production of antioxidant enzymes (34). Here, using young mice, we observed that global ROS levels did not significantly change in *Angptl2*$^{Flox/Flox}$*;MCK-Cre* mice compared with *Angptl2*$^{Flox/Flox}$ mice, but slightly decreased ROS levels were observed in some low-molecular-weight proteins (Fig. 2*d*). However, others have reported that global ROS levels induced by denervation significantly decrease in *Angptl2*$^{Flox/Flox}$*;MCK-Cre* mice related to *Angptl2*$^{Flox/Flox}$ mice (35). Consistent with these results, we found that *Angptl2* knockdown in differentiated C2C12 cells resulted in low ROS levels (Fig. 2*i*). Accordingly, catalase levels increased in both normal and denervated *Angptl2*$^{Flox/Flox}$*;MCK-Cre* mice

Figure 1. ANGPTL2 levels increase in skeletal muscle of aging mice. *a,* relative transcript levels of cellular senescence-associated (*p16*, *p19*, *p21*, and *p57*) and pro-inflammatory (*Il-1β* and *Il-6*) genes in musculus gastrocnemius and musculus soleus of adult (8-month-old) and aging (18-month-old) female wildtype mice ($n = 4$ per group). *b,* absolute muscle mass and body weight as well as tibia length normalized muscle mass in adult and aging mice ($n = 7$–10 per group). *c,* representative Western blot of 4-HNE-adducted proteins, a product of oxidative stress, in musculus soleus of adult and aging mice. *Asterisks* indicate increased levels of 4-HNE-adducted proteins in aging mice. *d–f,* relative expression of genes encoding antioxidant enzymes (catalase, *Sod1*, *Sod2*, and *Gpx1*) (*d*) or *Cd34*, *Pax3*, and *Pax7* (*e*), or *Angptl2* (*f*) transcripts in musculus gastrocnemius and musculus soleus of adult and aging mice ($n = 4$ per group). *g,* representative Western blot and the quantifications of ANGPTL2 and PAX7 proteins in musculus gastrocnemius and musculus soleus of adult and aging mice. *h,* representative Western blot of ANGPTL2 in SMC-rich or stromal cells-rich fractions isolated from musculus gastrocnemius of adult and aging mice. Myosin light chain (*MYL*) serves as a skeletal myocyte marker. Relative mRNA expression was normalized to 18S mRNA (*a, d, e,* and *f*). Hsc70 and CBB staining serves as an internal loading control (*c, g,* and *h*). Values in adult mice were set to 1 (*a* and *d–g*). All data are presented as means ± S.D. (*a, b,* and *d–f*) or means ± S.E. *g,* statistical significance was determined by Student's *t* test. *, $p < 0.05$; **, $p < 0.01$; †, $p < 0.001$.

as seen in *Angptl2*-knockdown differentiated C2C12 cells (Figs. 2, *e* and *j* and 5*c*). Overall, these results indicate that ANGPTL2-induced ROS accumulation may require catalase down-regulation.

Peroxisome proliferator-activated receptors (PPARs) reportedly play important roles in activating transcription of genes encoding antioxidant enzymes (36). Recent studies report that PPARα activates catalase expression and that PPARα expression decreases with age in tissues like skin and heart (37, 38). Moreover, our recent study showed that in cardiomyocytes, excess ANGPTL2 signaling down-regulates PPARα expression, whereas ANGPTL2 suppression up-regulates it (19). Taken together with findings reported here, we propose that excess ANGPTL2 signaling in aging skeletal

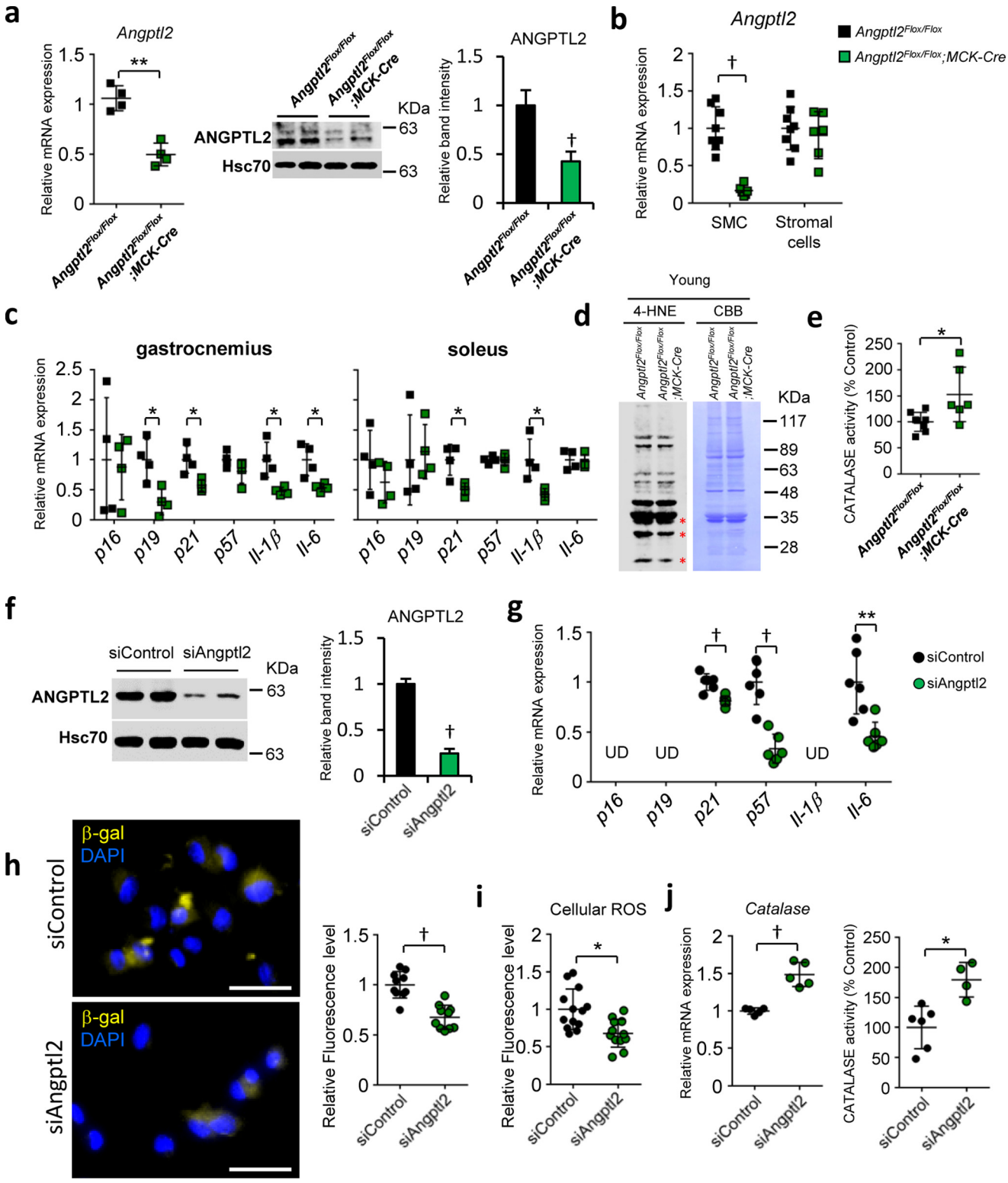

muscle may enhance ROS accumulation by decreasing PPARα-mediated catalase expression.

Here, we also report that Angptl2 loss in skeletal muscle decreases expression of genes associated with inflammation and cellular senescence. We previously reported that ANGPTL2 promotes chronic tissue inflammation by activating the integrin α5β1/nuclear factor-κB (NF-κB) pathway and through p38 MAPK activity (22, 39, 40). Therefore, we hypothesize that increased pro-inflammatory gene expression in skeletal muscle downstream of ANGPTL2 could be due to activation of these two pro-inflammatory pathways. Because inflammation and ROS induce cellular senescence (4, 5), ANGPTL2 may accelerate muscle cell senescence by promoting both. As noted above, ANGPTL2 is an SASP factor, and its expression increases in senescent cells (20, 21). Overall, up-regulated ANGPTL2 signaling in skeletal muscle cell may underlie inflammation, ROS accumulation, and cellular senescence.

In aging muscle, satellite cell self-renewal activity is reduced, and the number of quiescent satellite cells decreases (41). Moreover, differentiation of activated satellite cells and myotube formation are impaired in aging muscles (42). Interestingly, in young mice, ANGPTL2 suppression in skeletal myocytes increases the number of activated satellite cells without affecting quiescent satellite cell population, suggesting that ANGPTL2 deficiency in skeletal myocytes does not impair satellite cell self-renewal capacity. We also showed that decreased expression of several genes associated with both satellite cell activation and increased inflammation/ROS accumulation in a denervation-induced muscle atrophy mouse model is ameliorated by *Angptl2* knockout. Inflammation and ROS block activity of satellite cell precursors of skeletal muscle cells (14), suggesting that at least ANGPTL2 antagonizes satellite cell development via these mechanisms. Further studies are necessary to investigate whether ANGPTL2 directly modulates satellite cell function or whether suppression of ANGPTL2 production from skeletal myocytes could prevent or ameliorate sarcopenia development.

Activated satellite cells reportedly proliferate, differentiate into myocytes, and fuse in muscle fibers, increasing muscle mass (43). Here, we showed that exercise-induced ANGPTL2 suppression decreases inflammation and ROS accumulation and facilitates satellite cell activation. Taken together, these findings suggest that satellite cells activated by exercise-induced ANGPTL2 suppression in skeletal myocytes could generate muscle fibers and that their presence could present loss of muscle mass.

Exercise training, including running and walking, counteracts development of heart failure and sarcopenia in humans (15–17). We recently observed decreased ANGPTL2 expression in mouse heart tissues after exercise training through exercise-induced, cardiac miR-222-mediated ANGPTL2 suppression (19). We also found that inactivation of heart-derived autocrine/paracrine ANGPTL2 signaling protected mice from heart failure development (19). Interestingly, this study shows that exercise training also suppresses ANGPTL2 expression in skeletal muscle and that ANGPTL2 suppression antagonizes muscle fiber loss induced by denervation. It is noteworthy that exercise-induced ANGPTL2 suppression is a potential mechanism underlying exercise-associated prevention of sarcopenia development. Further studies are needed to determine how exercise training decreases ANGPTL2 expression in skeletal muscle on a mechanistic level.

We previously reported that circulating levels of ANGPTL2 increase with age in the general Japanese population and in mice (23). Interestingly, we found that in mice the age-dependent increases in serum ANGPTL2 concentration are suppressed by skeletal myocyte–specific ANGPTL2 deletion (Fig. S3*b*), suggesting that increased ANGPTL2 production from myocytes contributes in part to age-dependent increases in circulating levels of this factor.

In summary, this is the first study to report that increased ANGPTL2 produced from skeletal muscle may be a novel factor involved in promoting loss of muscular volume, enhancing inflammation and ROS accumulation, and suppressing satellite cell activity (Fig. 7, *left panel*). We also propose that exercise-induced ANGPTL2 suppression could reduce inflammation and ROS accumulation, facilitating satellite cell activation required to maintain muscle mass (Fig. 7, *right panel*).

Experimental procedures

Animal study

Male or female C57BL/6NJcl and female Angptl2 conditional knockout mice (*Angptl2*$^{Flox/Flox}$*;MCK-Cre* and *Angptl2*$^{Flox/Flox}$) were used in this study. MCK-Cre mice were purchased form The Jackson Laboratory. *Angptl2*$^{Flox/Flox}$ mice were described

Figure 2. *Angptl2* deficiency suppresses inflammation and cellular senescence and increases catalase activity in skeletal myocytes. *a–e* shows *in vivo* (skeletal muscles) analysis; *f–j* shows the *in vitro* (differentiated C2C12) analysis. *a,* relative mRNA expression (*left*) and representative Western blot (*middle*) and ANGPTL2 quantification in skeletal muscle of *Angptl2*$^{Flox/Flox}$*;MCK-Cre* mice and *Angptl2*$^{Flox/Flox}$ mice ($n = 4$ per group). *b,* relative *Angptl2* mRNA expression in skeletal myocyte (*SMC*)-rich or stromal cell-rich fractions isolated from musculus gastrocnemius of *Angptl2*$^{Flox/Flox}$*;MCK-Cre* mice and *Angptl2*$^{Flox/Flox}$ mice ($n = 6–8$ per group). *c,* relative expression of cellular senescence-associated or pro-inflammatory genes in musculus gastrocnemius and musculus soleus of *Angptl2*$^{Flox/Flox}$*;MCK-Cre* mice and *Angptl2*$^{Flox/Flox}$ mice ($n = 4$ per group). *d,* representative Western blot of 4-HNE-adducted proteins in musculus gastrocnemius of *Angptl2*$^{Flox/Flox}$*;MCK-Cre* and *Angptl2*$^{Flox/Flox}$ mice. *Asterisks* indicate decreased levels of these proteins seen in *Angptl2*$^{Flox/Flox}$*;MCK-Cre* mice. *e,* relative catalase activity in musculus gastrocnemius of *Angptl2*$^{Flox/Flox}$*;MCK-Cre* and *Angptl2*$^{Flox/Flox}$ mice ($n = 6–8$ per group). *f,* representative Western blot and the quantification of *ANGPTL2* expression in differentiated C2C12 cells transfected with siRNA control (siControl) or siRNA Angptl2 (siAngptl2) ($n = 3$ per group for ANGPTL2 quantification). *g,* relative transcript levels of cellular senescence-associated genes in differentiated C2C12 cells transfected with Angptl2 or control siRNA (*UD,* undetected) ($n = 6$ per group). *h,* representative images and relative fluorescence levels of SPiDER-βgal staining of differentiated C2C12 cells transfected with Angptl2 or control siRNA (*scale bar,* 50 μm) ($n = 10$ per group). *i,* relative fluorescence levels detected by CM-H2DCFDA (general oxidative stress indicator) of differentiated C2C12 cells transfected with Angptl2 or control siRNA ($n = 12–13$ per group). *j,* relative catalase transcript levels (*left*) or activity (*right*) in differentiated C2C12 cells transfected with Angptl2 or control siRNA ($n = 5–6$ per group). Relative mRNA expression was normalized to 18S mRNA (*a–c, g,* and *j*). Hsc70 and CBB serve as internal loading controls (*a, d,* and *f*). Values in *Angptl2*$^{Flox/Flox}$ mice were set to 1 (*a–c, e–g,* and *i–g*). All data are presented as means ± S.D. (*a, left, b, c, e,* and *g–j*) or means ± S.E. (*a, right,* and *f*); statistical significance was determined by Student's *t* test. *, $p < 0.05$; **, $p < 0.01$; †, $p < 0.001$.

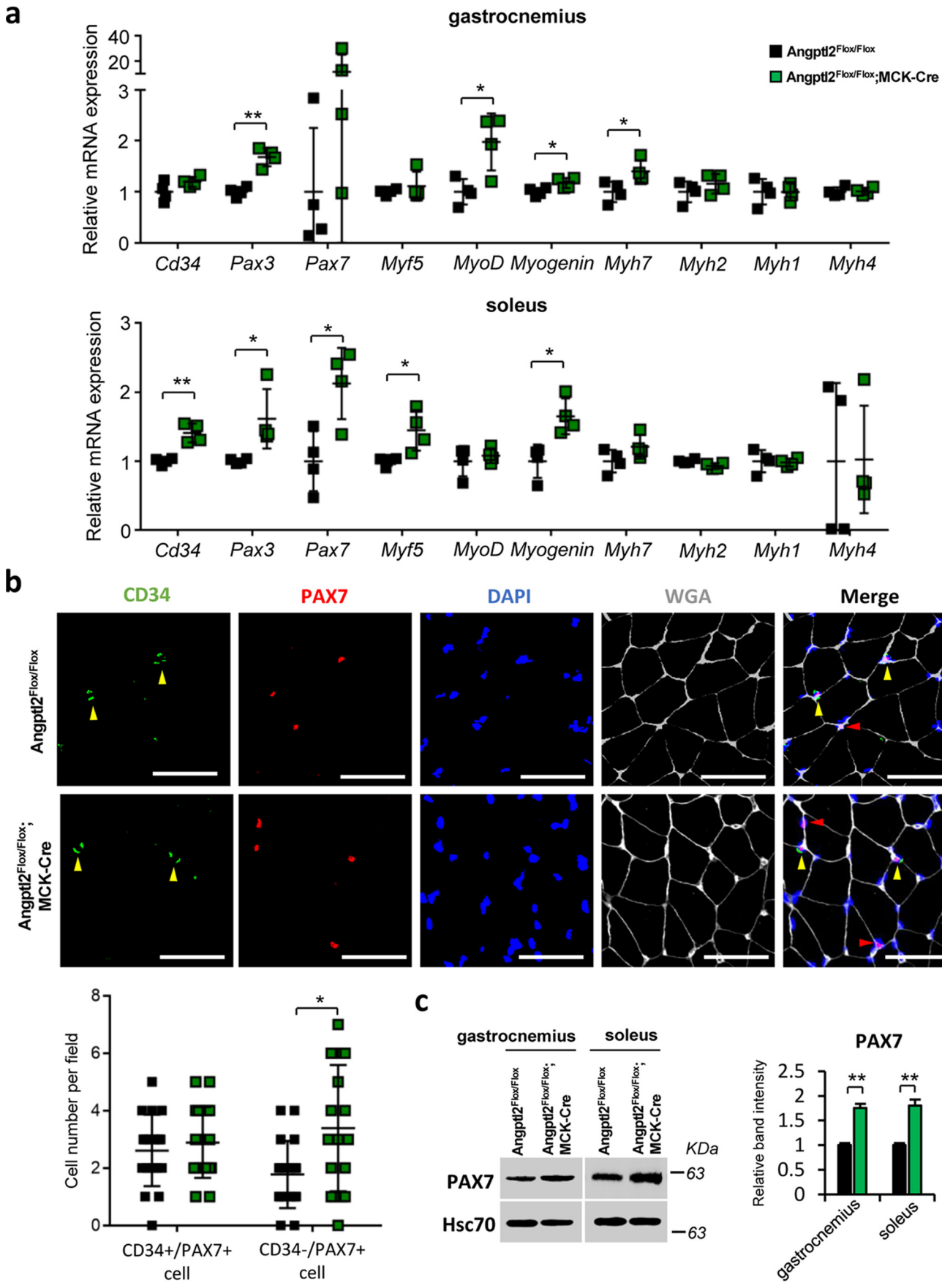
a
gastrocnemius
Angptl2Flox/Flox
Angptl2Flox/Flox;MCK-Cre
Relative mRNA expression
Cd34 Pax3 Pax7 Myf5 MyoD Myogenin Myh7 Myh2 Myh1 Myh4
soleus
b
CD34
PAX7
DAPI
WGA
Merge
Angptl2Flox/Flox
Angptl2Flox/Flox; MCK-Cre
Cell number per field
CD34+/PAX7+ cell
CD34-/PAX7+ cell
c
gastrocnemius
soleus
KDa
PAX7
Hsc70
63
Relative band intensity
gastrocnemius
soleus

previously (19). Mice were fed a normal diet and water *ad libitum*, bred in a mouse house with automatically controlled lighting (12 h on, 12 h off), and maintained at a stable temperature of 23 °C. All experimental procedures were approved by the Kumamoto University Ethics Review Committee for Animal Experimentation.

Mouse denervation-induced muscle atrophy model

Twelve-week-old female *Angptl2$^{Flox/Flox}$;MCK-Cre* mice were anesthetized by intraperitoneal injection with sodium pentobarbital. The sciatic nerve of the left hindlimb was excised ~0.5–1 cm, whereas the sciatic nerve of the contralateral hindlimb was sham-operated by exposure without excision. At 3, 7, and 14 days after denervation, mice were sacrificed for analysis.

Exercise training

Exercise was performed as described previously (19). Briefly, 12-week-old male mice were exposed to a treadmill chamber with free movement for environmental adaptation for 30 min before the exercise. Mice were then trained using the following protocol: 5 m/min for 5 min, 10 m/min for 5 min, 15 m/min for 5 min, and 20 m/min for 60 min. These mice were sacrificed immediately or 3 h after exercise. A different group of endurance-trained mice were trained for 2 weeks (5 days/week) and were sacrificed 3 h after the last run.

Isolation of skeletal muscle myofibers and non-myofibers

Isolation followed a previously described protocol (44). Briefly, as shown in Fig. S2*a*, gastrocnemius muscle was dissected and incubated in collagenase solution (L-15 medium (1601301, Gibco™ Life Technologies, Inc.) containing 500 units/ml collagenase type I (CLS1, Worthington)) at 37 °C for 2 h. Muscle was transferred to pre-warmed PBS and then flushed with PBS using a pipette under a microscope until myofibers were isolated. The entire solution was then collected and passed in turn through 100- and 40-μm mesh filters. The filtrate was collected into a new Falcon tube and centrifuged at 3000 rpm for 5 min to collect non-myofibers. The 100-μm mesh filter was flushed with pre-warmed PBS from the underside, and the flushed fluid was transferred to a new Falcon tube and centrifuged as above to collect myofibers. The supernatant was discarded, and the pellet was subjected to RNA extraction or to Western analysis.

C2C12 culture and AICAR treatment

C2C12 cells were cultured in Dulbecco's modified Eagle's medium (DMEM; WAKO 044-29765, Tokyo, Japan) supplemented with 10% fetal calf serum in a humidified atmosphere with 5% CO_2 at 37 °C. Cells reached to 60–80% confluence after being seeded for 24 h and then the medium was replaced by DMEM containing 2% horse serum for 96 h to induce differentiation. All *in vitro* studies reported here were conducted in differentiated C2C12 cells. Differentiated C2C12 cells for knockdown analysis were established using Mission siRNA Universal Negative Control (siControl, Sigma) or Mission siRNA targeting *Angptl2* (siAngptl2: SASI_Mn01_00095185: 5′-GAGAGUACAUUUACCUCAATT-3′. Sigma). Cells were transfected using Lipofectamine™ RNAiMAX transfection reagent (13778-150, Invitrogen). For AICAR treatment, differentiated C2C12 cells were incubated with 1 mM AICAR (A9978, Sigma) for 1, 6, or 12 h.

ANGPTL2 ELISA

A human ANGPTL2 assay kit-IBL (27745; Immuno-Biological Laboratories, Gunma, Japan) was used to measure ANGPTL2 concentration in supernatants or in mouse serum in accordance with the manufacturer's instructions. Briefly, supernatants were diluted 10-fold with EIA buffer, and 100 μl of the sample was placed into wells of a tissue culture plate. Samples were incubated 60 min at 37 °C, washed four times with the washing buffer provided, and then treated with labeled antibody solution and incubated another 30 min at 4 °C. Samples were then washed five times and then treated with 3,3′,5,′-tetramethylbenzidine (TMB) solution for 30 min at room temperature protected from light. After addition of stop solution, plates were then analyzed for absorbance at $A_{450\ nm}$ using an iMark™ microplate reader (168-1130 JA, Bio-Rad).

Catalase activity assay

Catalase activity was measured using a catalase activity assay kit (ab83464, Abcam, Cambridge, UK) according to the manufacturer's instructions. Briefly, C2C12 cells or skeletal muscle tissues were homogenized in assay buffer and purified. Standards, the positive control, the sample, or the sample high control were added to 96-well plate in volumes described in the manufacturer's instructions prior to addition of the reagent. Absorbance at $A_{595\ nm}$ was measured using an iMark™ microplate reader (168-1130 JA, Bio-Rad), and catalase activity was calculated using formulas supplied by the manufacturer (Abcam, Cambridge, UK).

ROS detection

C2C12 cellular ROS was detected using CM-H2DCFDA reagent (General Oxidative Stress Indicator) (C6827, Invitrogen) based on the manufacturer's instructions. Briefly, cells were seeded in a 96-well microplate and incubated for 30 min at

Figure 3. *Angptl2* deficiency in skeletal myocytes enhances satellite cell activity. *a,* relative transcript levels of satellite cell activation-associated genes (*Cd34*, *Pax3*, *Pax7*, *Myf5*, *MyoD*, and myogenin) and skeletal muscle myosin subtypes (*Myh1*, *Myh2*, *Myh4*, and *Myh7*) in musculus gastrocnemius and musculus soleus of *Angptl2$^{Flox/Flox}$;MCK-Cre* or *Angptl2$^{Flox/Flox}$* mice ($n = 4$ per group). *b,* representative immunostaining and quantifications of CD34 (*green*) and PAX7 (*red*) in musculus gastrocnemius of *Angptl2$^{Flox/Flox}$;MCK-Cre* or *Angptl2$^{Flox/Flox}$* mice. Myofibers are co-stained with DAPI (*blue*) and WGA (*gray*). *Yellow arrowheads* in *Merge* indicate CD34- and PAX7-positive cells. *Red arrowheads* in *Merge* indicate PAX7-positive cells. (*Scale bar,* 50 μm. Six different fields are quantified per mouse, $n = 3$ per group.) *c,* representative Western blot and PAX7 quantification in musculus gastrocnemius and musculus soleus of *Angptl2$^{Flox/Flox}$;MCK-Cre* and *Angptl2$^{Flox/Flox}$* mice. Hsc70 serves as the internal loading control. Values in *Angptl2$^{Flox/Flox}$* mice were set to 1 (*a* and *c*). All data are presented as means ± S.D. (*a* and *b*) or means ± S.E. (*c*); statistical significance was determined by Student's *t* test. *, $p < 0.05$; **, $p < 0.01$.

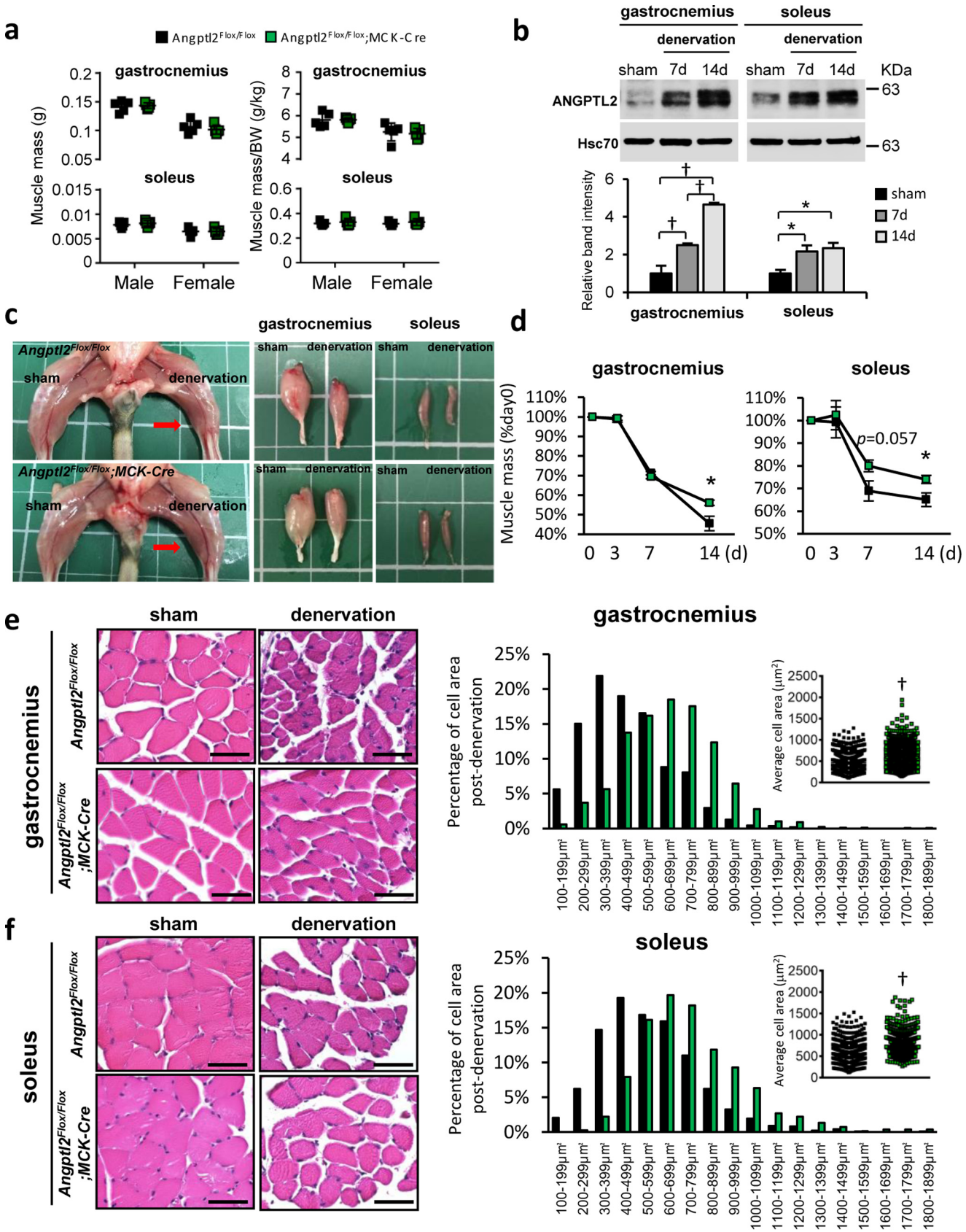
a
Angptl2Flox/Flox
Angptl2Flox/Flox;MCK-Cre
gastrocnemius
soleus
Muscle mass (g)
Muscle mass/BW (g/kg)
Male
Female
b
gastrocnemius
soleus
denervation
sham
7d
14d
KDa
ANGPTL2
Hsc70
63
Relative band intensity
c
gastrocnemius
soleus
Angptl2Flox/Flox
Angptl2Flox/Flox;MCK-Cre
sham
denervation
d
gastrocnemius
soleus
Muscle mass (%day0)
p=0.057
0 3 7 14 (d)
e
sham
denervation
gastrocnemius
Angptl2Flox/Flox
Angptl2Flox/Flox;MCK-Cre
Percentage of cell area post-denervation
Average cell area (μm²)
100-199μm²
200-299μm²
300-399μm²
400-499μm²
500-599μm²
600-699μm²
700-799μm²
800-899μm²
900-999μm²
1000-1099μm²
1100-1199μm²
1200-1299μm²
1300-1399μm²
1400-1499μm²
1500-1599μm²
1600-1699μm²
1700-1799μm²
1800-1899μm²
f
soleus

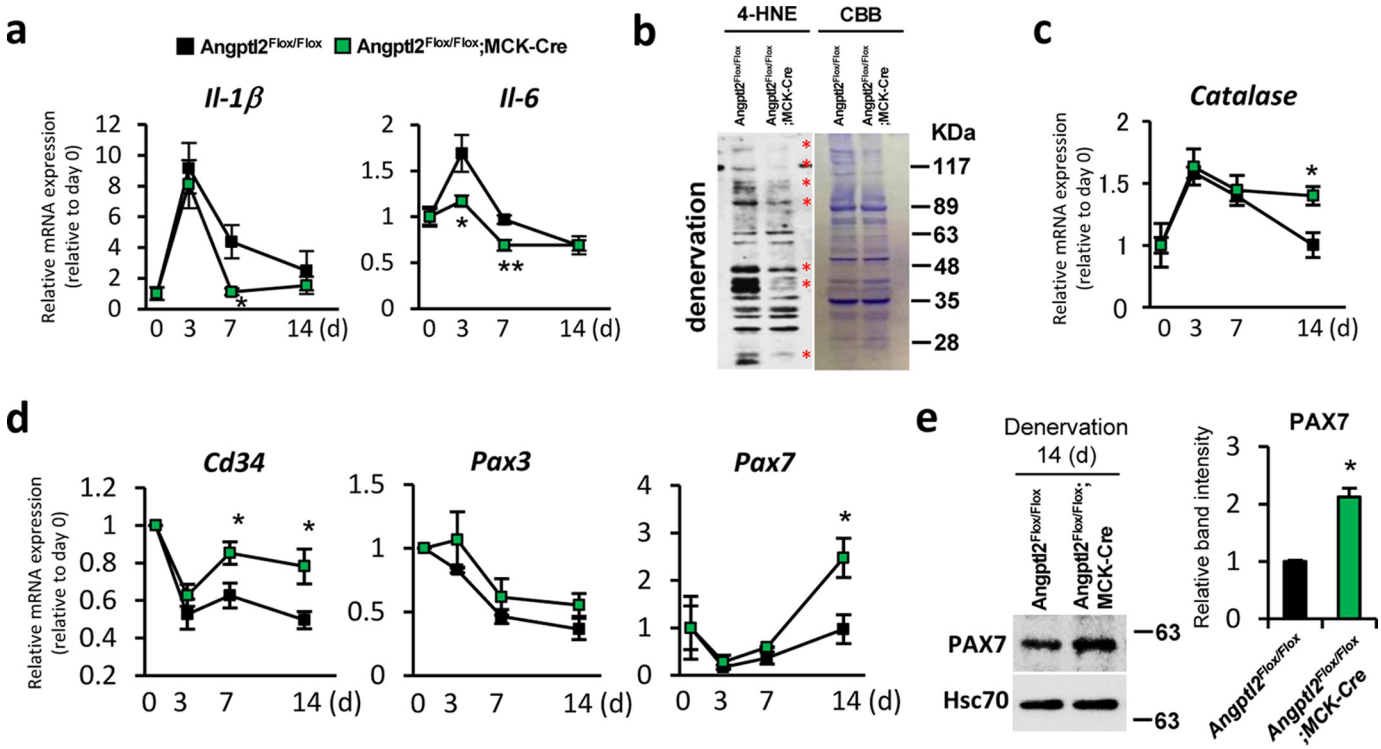

Figure 5. *Angptl2*-deficient skeletal myocytes show decreased inflammation and ROS levels and increased satellite cell activity. *a, c,* and *d,* relative expression of *Il-1β*, *Il-6* (*a*), catalase (*c*), and satellite cell activation-associated (*d*) mRNAs in denervated musculus gastrocnemius of *Angptl2*$^{Flox/Flox}$*;MCK-Cre* or *Angptl2*$^{Flox/Flox}$ mice ($n = 5$ per group). Relative mRNA expression was normalized to 18S mRNA. *b,* representative Western blot of 4-HNE-adducted proteins in denervated musculus gastrocnemius of *Angptl2*$^{Flox/Flox}$*;MCK-Cre* or *Angptl2*$^{Flox/Flox}$ mice. *Asterisks* indicate decreased levels of these proteins seen in *Angptl2*$^{Flox/Flox}$*;MCK-Cre* mice. *e,* representative Western blot and PAX7 quantification 14 days after denervation in musculus gastrocnemius of *Angptl2*$^{Flox/Flox}$*; MCK-Cre* or *Angptl2*$^{Flox/Flox}$ mice. Hsc70 and CBB serve as internal loading controls (*b* and *e*). Values at day 0 of denervation in both *Angptl2*$^{Flox/Flox}$*;MCK-Cre* and *Angptl2*$^{Flox/Flox}$ mice (*a, c,* and *d*) and in *Angptl2*$^{Flox/Flox}$ mice (*e*) were set to 1. All data are presented as means ± S.E. (*a, c,* and *d*) or means ± S.D. (*e*); statistical significance was determined by Student's *t* test. *, $p < 0.05$; **, $p < 0.01$.

37 °C with 10 μM CM-H2DCFDA and then washed twice with PBS. Cellular ROS levels were then detected at an excitation/emission of 485/515 nm using a Fluoroskan Ascent Microplate Luminometer (Thermo Fisher Scientific Inc., Carlsbad, CA). Data were analyzed using Ascent software (Version 2.6). Skeletal muscular ROS levels were assessed by examining the 4-HNE-adducted protein levels in skeletal muscle samples (see under "Western blotting").

SPiDER-βgal staining

SPiDER-βgal reagent (SG02, DOJINDO, Kumamoto, Japan) was used for cellular βgal staining based on the manufacturer's instructions. Briefly, cells were seeded on 96-well microplates or chamber slides (SCS-002, Matsunami, Osaka, Japan) for differentiation. After Angptl2 knockdown, 1μmol/liter SPiDER-βgal working solution was added and incubated for 15 min at 37 °C protected from light. After 2 washes with PBS, cells were evaluated using a Fluoroskan Ascent Microplate Luminometer (Thermo Fisher Scientific Inc.) or images were obtained using a fluorescence microscope (model BZ-9000; Keyence, Osaka, Japan).

Cellular mechanical stretch

C2C12 cells were seeded on BIOFLEX®PLATE COLLAGEN I-BF 3001C (Flexcell® International Corp., Burlington, NC) plates. After differentiation, cells were subjected to 5, 10, or 15% elongation with 1 Hz sine wave cyclic stretch for 15 or 30 min. Control cells were not subjected to stretch. Cells were then harvested and immediately analyzed.

Histological staining

For routine hematoxylin and eosin (HE) staining, skeletal muscle was dissected, fixed in 4% formalin for >12 h at room temperature, then embedded in paraffin, and cut into 5-μm-thick sections. Images were obtained using a fluorescence microscope (model BZ-9000; Keyence, Osaka, Japan). The area

Figure 4. *Angptl2* deficiency in skeletal myocytes prevents skeletal muscle atrophy. *a,* absolute muscle mass and body weight normalized muscle mass in musculus gastrocnemius and musculus soleus of normal *Angptl2*$^{Flox/Flox}$*;MCK-Cre* or *Angptl2*$^{Flox/Flox}$ male or female mice ($n = 5$ per group). *b,* representative Western blot and ANGPTL2 quantification in musculus gastrocnemius and musculus soleus of wildtype mice after denervation surgery ($n = 4$ per group). Hsc70 serves as an internal loading control. *c,* representative images of lower limbs and samples of musculus gastrocnemius and musculus soleus from sham-operated or 2-week-denervated *Angptl2*$^{Flox/Flox}$*;MCK-Cre* or *Angptl2*$^{Flox/Flox}$ mice. *Red arrow* indicates atrophied muscle. *d,* muscle mass is shown as a percentage of the day 0 value of denervated musculus gastrocnemius and musculus soleus in *Angptl2*$^{Flox/Flox}$*;MCK-Cre* or *Angptl2*$^{Flox/Flox}$ mice ($n = 5$ per group). *e* and *f,* representative HE staining images (*left*) and cross-sections of myofibers (*right*) in musculus gastrocnemius (*e*) and musculus soleus (*f*) of sham-operated or 2-week-denervated *Angptl2*$^{Flox/Flox}$*;MCK-Cre* or *Angptl2*$^{Flox/Flox}$ mice. (*Scale bar,* 50 mm. $n = 5$, $n = 1200–1700$ per group for gastrocnemius, $n = 800–1000$ per group for soleus.) Values in sham mice were set to 1 (*b*). All data are presented as means ± S.D. (*a, e,* and *f*) or means ± S.E. (*b* and *d*); statistical significance was determined by Student's *t* test (*a* and *d–f*) or one-way ANOVA (*b*), *, $p < 0.05$; †, $p < 0.001$.

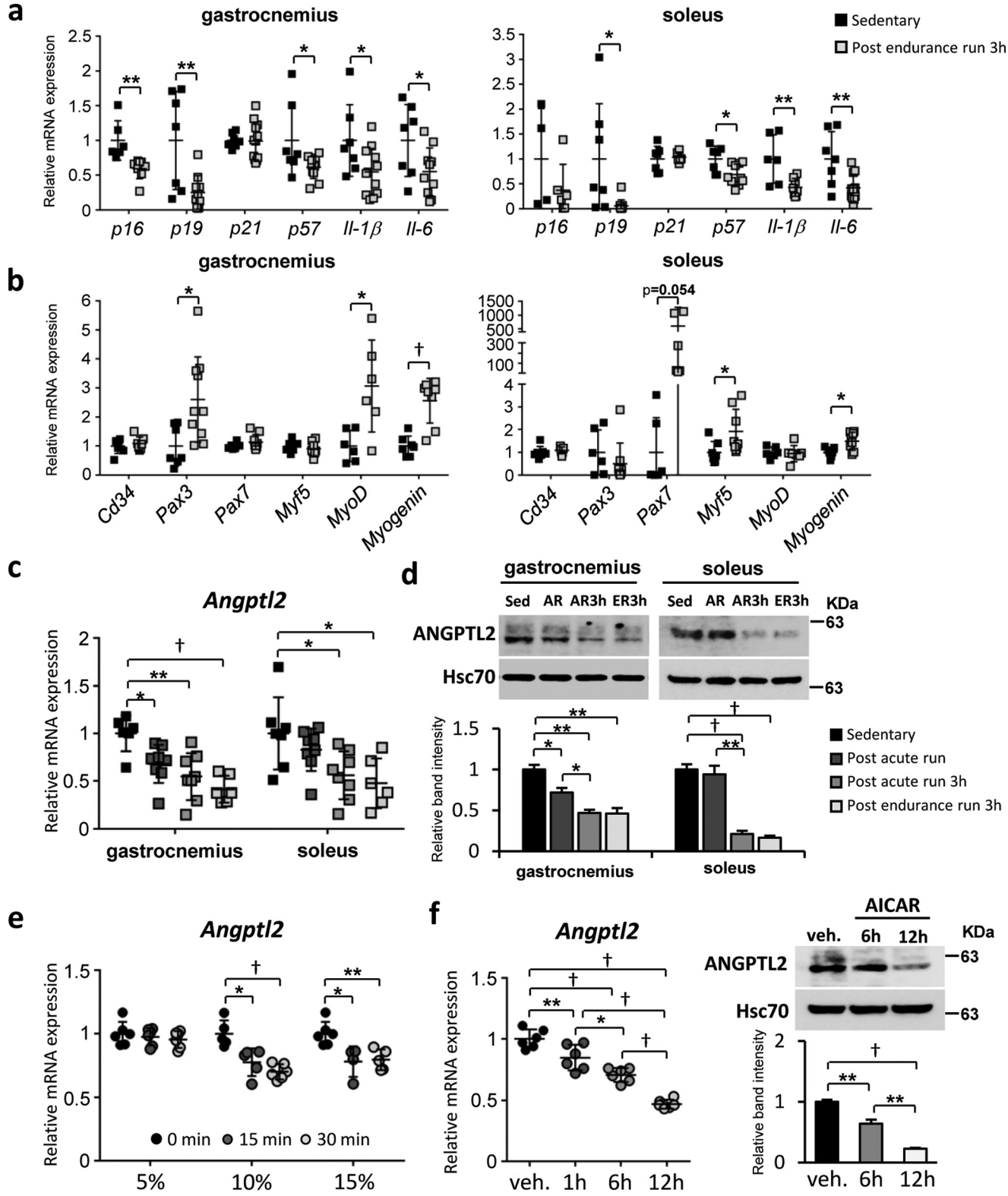

Figure 6. Exercise training suppresses *Angptl2* expression in skeletal muscles. *a–d* show *in vivo* (skeletal muscles) analysis; *e* and *f* show *in vitro* (differentiated C2C12) analysis. *a* and *b*, relative transcript levels of markers of senescence and pro-inflammation (*a*) and satellite cells (*b*) in musculus gastrocnemius and musculus soleus of wildtype mice, 3 h after an endurance run ($n = 7–12$ per group). *c* and *d*, relative *Angptl2* mRNA (*c*) and protein (*d*) expression in musculus gastrocnemius and musculus soleus of wildtype C57BL/6NJcl male mice after exercise training. (*Sed*, sedentary; *AR*, post-acute run; *AR3h*, post-acute run plus 3 h; *ER3h*, post-endurance run plus 3 h.) ($n = 6–8$ per group for *c*; $n = 3–4$ per group for *d*.) *e*, relative *Angptl2* mRNA expression in differentiated C2C12 cells exposed to mechanical stretch by 5, 10, or 15% extension with 1 Hz sine wave cycle for 15 or 30 min ($n = 4–6$ per group). *f*, relative *Angptl2* mRNA (*left*) and protein (*right*) expression in differentiated C2C12 cells treated with 1 mM AICAR for indicated time points (1, 6, and 12 h) ($n = 6$ per group). Relative mRNA expression was normalized to 18S mRNA (*a–c*, *e* and *f*). Hsc70 serves as the internal loading control (*d* and *f*). Values in sedentary mice (*a–d*), in the 0-min group (*e*) and in the vehicle (*veh*) group (*f*) were set to 1. All data are presented as means ± S.D. (*a–c*, *e*, and *f*, *left*) or means ± S.E. (*d* and *f*, *right*); statistical significance was determined by Student's *t* test (*a* and *b*) or one-way ANOVA (*c* and *d–f*). *, $p < 0.05$; **, $p < 0.01$; †, $p < 0.001$.

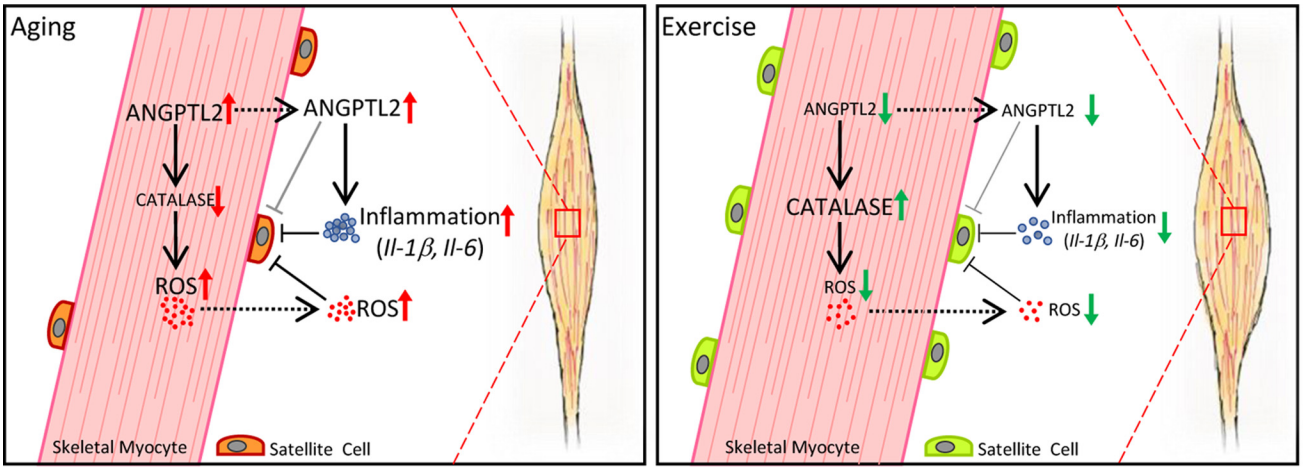

Figure 7. Model of ANGPTL2 activity in skeletal muscle. *Left, ANGPTL2* expression in skeletal myocytes increases with age. Skeletal myocyte-derived ANGPTL2 promotes inflammation and facilitates ROS accumulation by decreasing catalase expression in skeletal muscle. Increased ANGPTL2 and associated inflammation and ROS accumulation impair satellite cell activity in skeletal muscle, leading to atrophy. *Right,* exercise training decreases *ANGPTL2* expression in skeletal muscle as it suppresses inflammation and ROS accumulation. These activities facilitate satellite cell activation that contribute to maintenance of muscle mass. Thus, exercise training-induced ANGPTL2 down-regulation represents a potential mechanism underlying exercise-induced protection from muscle atrophy.

of each cellular cross-section was analyzed using BZ-X analyzer software (Keyence, Osaka, Japan).

For immunofluorescence, we used frozen sections of skeletal muscle. Sections were fixed with cold acetone for 20 min and blocked with 5% goat serum for 20 min at room temperature. The primary antibody was incubated at 4 °C overnight, and then second antibodies or wheat germ agglutinin (WGA) were incubated at room temperature for 1 h. Antibodies used in immunofluorescence were as follows: anti-CD34 (1:50, 13-0341-85, RAM34, eBioscience, Carlsbad, CA); anti-Pax7 (1:20, PA1-117, Invitrogen); WGA (W11262, Invitrogen). Image was obtained from confocal microscopy (FV1200 IX83, OLYMPUS, Tokyo, Japan) and quantified by ImageJ.

RT-PCR

Total RNA was isolated from C2C12 cells or skeletal muscle using an RNeasy mini kit (Qiagen, Valencia, CA). mRNA was converted to cDNA using a Prime Script RT reagent kit (Takara Bio Inc., Shiga, Japan). PCRs were performed in a Thermal Cycler Dice Real-Time System TP870 (Takara Bio Inc., Shiga, Japan) using SYBR Premix EX Taq (Takara Bio Inc., Shiga, Japan) according to the manufacturer's instructions. Relative gene expression was determined using the standard curve method, and fold-changes of targeted genes were normalized to 18S mRNA. Primer sequences used are shown in Table S1.

Western blotting

Differentiated C2C12 cells or skeletal muscle tissues were homogenized in lysis buffer (10 mM Tris-HCl, 1% Triton X-100, 50 mM NaCl, 30 mM sodium pyrophosphate, 50 mM NaF, 5 mM EDTA, 0.1 mM Na_3VO_4, plus a protease inhibitor mixture (Nacalai Tesque, Kyoto, Japan), pH 7.5). SDS-PAGE was performed on gradient gels (SuperSep™Ace, 5–20%, 17-well, WAKO, Tokyo, Japan), and immunoblotting was performed as described (19). Antibodies for anti-Angptl2 (BAF1444; R&D Systems, Minneapolis, MN), anti-Pax7 (PAX7497, Abcam, Cambridge, UK), anti-4-HNE (MAB3249, R&D Systems, Minneapolis, MN), anti-MYL (F-5, sc-365243; Santa Cruz Biotechnology, Dallas, TX), and anti-Hsc70 (sc-7298; Santa Cruz Biotechnology) were used. CBB staining was performed using Quick-CBB reagent (299-50101, WAKO, Tokyo, Japan). Briefly, after image acquisition, the PVDF membrane was washed with TBST and incubated 15 min with stripping buffer (46430, Thermo Fisher Scientific Inc.), followed by washing 5 min three times in TBST. Membranes were dipped into the Quick-CBB reagent mixture (solution A + solution B) for 20 min, washed with deionized water 4–6 times, and imaged.

Statistical analyses

All data are represented as the means ± S.D. or means ± S.E. of the mean. Statistical significance of two group comparisons of variables was determined using Student's *t* test, and multiple comparisons were assessed by one- or two-way ANOVA. $p < 0.05$ was considered statistically significant.

Author contributions—J. Z., Z. T., and Y. O. conceived the study and designed the experiments. J. Z., Z. T., P. X., and K. M. performed experiments and collected or analyzed data. T. Y. and K. Y. provided instructions and assisted with the cellular stretch experiment. J. Z., Z. T., T. K., and Y. O. wrote the paper. K. M., T. S., M. E., S. Z., H. F., H. H., J. M., and K. T. provided necessary assistance.

Acknowledgments—We thank our colleagues for valuable suggestions and discussions. We also thank K. Tabu, M. Nakata, S. Iwaki, Y. Shougenji, and N. Shirai for technical assistance.

References

1. Seene, T., Kaasik, P., and Riso, E. M. (2012) Review on aging, unloading and reloading: changes in skeletal muscle quantity and quality. *Arch. Gerontol. Geriatr.* **54,** 374–380 CrossRef Medline
2. Degens, H., and Alway, S. E. (2006) Control of muscle size during disuse, disease, and aging. *Int. J. Sports Med.* **27,** 94–99 CrossRef Medline
3. Schaap, L. A., Pluijm, S. M., Deeg, D. J., and Visser, M. (2006) Inflammatory markers and loss of muscle mass (sarcopenia) and strength. *Am. J. Med.* **119,** 526 e529–e517 CrossRef Medline

4. Jo, E., Lee, S. R., Park, B. S., and Kim, J. S. (2012) Potential mechanisms underlying the role of chronic inflammation in age-related muscle wasting. *Aging Clin. Exp. Res.* **24,** 412–422 Medline
5. Finkel, T., and Holbrook, N. J. (2000) Oxidants, oxidative stress and the biology of ageing. *Nature* **408,** 239–247 CrossRef Medline
6. Giorgio, M., Trinei, M., Migliaccio, E., and Pelicci, P. G. (2007) Hydrogen peroxide: a metabolic by-product or a common mediator of ageing signals? *Nat. Rev. Mol. Cell Biol.* **8,** 722–728 CrossRef Medline
7. Fulle, S., Protasi, F., Di Tano, G., Pietrangelo, T., Beltramin, A., Boncompagni, S., Vecchiet, L., and Fanò, G. (2004) The contribution of reactive oxygen species to sarcopenia and muscle ageing. *Exp. Gerontol.* **39,** 17–24 CrossRef Medline
8. Zuo, L., Christofi, F. L., Wright, V. P., Liu, C. Y., Merola, A. J., Berliner, L. J., and Clanton, T. L. (2000) Intra- and extracellular measurement of reactive oxygen species produced during heat stress in diaphragm muscle. *Am. J. Physiol. Cell Physiol* **279,** C1058–C1066 Medline
9. Goodman, M. N. (1994) Interleukin-6 induces skeletal muscle protein breakdown in rats. *Proc. Soc. Exp. Biol. Med.* **205,** 182–185 CrossRef Medline
10. Sung, J. Y., Hong, J. H., Kang, H. S., Choi, I., Lim, S. D., Lee, J. K., Seok, J. H., Lee, J. H., and Hur, G. M. (2000) Methotrexate suppresses the interleukin-6 induced generation of reactive oxygen species in the synoviocytes of rheumatoid arthritis. *Immunopharmacology* **47,** 35–44 CrossRef Medline
11. Wang, P., Li, N., Li, J. S., and Li, W. Q. (2002) The role of endotoxin, TNF-α, and IL-6 in inducing the state of growth hormone insensitivity. *World J. Gastroenterol.* **8,** 531–536 CrossRef Medline
12. Schultz, E. (1989) Satellite cell behavior during skeletal muscle growth and regeneration. *Med. Sci. Sports Exerc.* **21,** S181–S186 Medline
13. Snijders, T., and Parise, G. (2017) Role of muscle stem cells in sarcopenia. *Curr. Opin. Clin. Nutr. Metab. Care* **20,** 186–190 CrossRef Medline
14. Palacios, D., Mozzetta, C., Consalvi, S., Caretti, G., Saccone, V., Proserpio, V., Marquez, V. E., Valente, S., Mai, A., Forcales, S. V., Sartorelli, V., and Puri, P. L. (2010) TNF/p38alpha/polycomb signaling to Pax7 locus in satellite cells links inflammation to the epigenetic control of muscle regeneration. *Cell Stem Cell* **7,** 455–469 CrossRef Medline
15. Woods, J. A., Wilund, K. R., Martin, S. A., and Kistler, B. M. (2012) Exercise, inflammation and aging. *Aging Dis.* **3,** 130–140 Medline
16. Radák, Z., Naito, H., Kaneko, T., Tahara, S., Nakamoto, H., Takahashi, R., Cardozo-Pelaez, F., and Goto, S. (2002) Exercise training decreases DNA damage and increases DNA repair and resistance against oxidative stress of proteins in aged rat skeletal muscle. *Pflugers Arch.* **445,** 273–278 CrossRef Medline
17. Hawke, T. J. (2005) Muscle stem cells and exercise training. *Exerc. Sport Sci. Rev.* **33,** 63–68 CrossRef Medline
18. Endo, M., Nakano, M., Kadomatsu, T., Fukuhara, S., Kuroda, H., Mikami, S., Hato, T., Aoi, J., Horiguchi, H., Miyata, K., Odagiri, H., Masuda, T., Harada, M., Horio, H., Hishima, T., *et al.* (2012) Tumor cell-derived angiopoietin-like protein ANGPTL2 is a critical driver of metastasis. *Cancer Res.* **72,** 1784–1794 CrossRef Medline
19. Tian, Z., Miyata, K., Kadomatsu, T., Horiguchi, H., Fukushima, H., Tohyama, S., Ujihara, Y., Okumura, T., Yamaguchi, S., Zhao, J., Endo, M., Morinaga, J., Sato, M., Sugizaki, T., Zhu, S., *et al.* (2016) ANGPTL2 activity in cardiac pathologies accelerates heart failure by perturbing cardiac function and energy metabolism. *Nat. Commun.* **7,** 13016 CrossRef Medline
20. Farhat, N., Thorin-Trescases, N., Voghel, G., Villeneuve, L., Mamarbachi, M., Perrault, L. P., Carrier, M., and Thorin, E. (2008) Stress-induced senescence predominates in endothelial cells isolated from atherosclerotic chronic smokers. *Can. J. Physiol. Pharmacol.* **86,** 761–769 CrossRef Medline
21. Shimamoto, A., Kagawa, H., Zensho, K., Sera, Y., Kazuki, Y., Osaki, M., Oshimura, M., Ishigaki, Y., Hamasaki, K., Kodama, Y., Yuasa, S., Fukuda, K., Hirashima, K., Seimiya, H., Koyama, H., *et al.* (2014) Reprogramming suppresses premature senescence phenotypes of Werner syndrome cells and maintains chromosomal stability over long-term culture. *PLoS ONE* **9,** e112900 CrossRef Medline
22. Tabata, M., Kadomatsu, T., Fukuhara, S., Miyata, K., Ito, Y., Endo, M., Urano, T., Zhu, H. J., Tsukano, H., Tazume, H., Kaikita, K., Miyashita, K., Iwawaki, T., Shimabukuro, M., Sakaguchi, K., *et al.* (2009) Angiopoietin-like protein 2 promotes chronic adipose tissue inflammation and obesity-related systemic insulin resistance. *Cell Metab.* **10,** 178–188 CrossRef Medline
23. Horio, E., Kadomatsu, T., Miyata, K., Arai, Y., Hosokawa, K., Doi, Y., Ninomiya, T., Horiguchi, H., Endo, M., Tabata, M., Tazume, H., Tian, Z., Takahashi, O., Terada, K., Takeya, M., *et al.* (2014) Role of endothelial cell-derived angptl2 in vascular inflammation leading to endothelial dysfunction and atherosclerosis progression. *Arterioscler. Thromb. Vasc. Biol.* **34,** 790–800 CrossRef Medline
24. Tian, Z., Miyata, K., Tazume, H., Sakaguchi, H., Kadomatsu, T., Horio, E., Takahashi, O., Komohara, Y., Araki, K., Hirata, Y., Tabata, M., Takanashi, S., Takeya, M., Hao, H., Shimabukuro, M., *et al.* (2013) Perivascular adipose tissue-secreted angiopoietin-like protein 2 (Angptl2) accelerates neointimal hyperplasia after endovascular injury. *J. Mol. Cell. Cardiol.* **57,** 1–12 CrossRef Medline
25. Poli, G., and Schaur, R. J. (2000) 4-Hydroxynonenal in the pathomechanisms of oxidative stress. *IUBMB Life* **50,** 315–321 CrossRef Medline
26. Jang, Y. C., Sinha, M., Cerletti, M., Dall'Osso, C., and Wagers, A. J. (2011) Skeletal muscle stem cells: effects of aging and metabolism on muscle regenerative function. *Cold Spring Harb. Symp. Quant. Biol.* **76,** 101–111 CrossRef Medline
27. Beyer, I., Mets, T., and Bautmans, I. (2012) Chronic low-grade inflammation and age-related sarcopenia. *Curr. Opin. Clin. Nutr. Metab. Care* **15,** 12–22 CrossRef Medline
28. Jejurikar, S. S., and Kuzon, W. M., Jr. (2003) Satellite cell depletion in degenerative skeletal muscle. *Apoptosis* **8,** 573–578 CrossRef Medline
29. Aagaard, P., Suetta, C., Caserotti, P., Magnusson, S. P., and Kjaer, M. (2010) Role of the nervous system in sarcopenia and muscle atrophy with aging: strength training as a countermeasure. *Scand. J. Med. Sci. Sports* **20,** 49–64 CrossRef Medline
30. Montero-Fernández, N., and Serra-Rexach, J. A. (2013) Role of exercise on sarcopenia in the elderly. *Eur. J. Phys. Rehabil. Med.* **49,** 131–143 Medline
31. Frontera, W. R., Meredith, C. N., O'Reilly, K. P., Knuttgen, H. G., and Evans, W. J. (1988) Strength conditioning in older men: skeletal muscle hypertrophy and improved function. *J. Appl. Physiol.* **64,** 1038–1044 Medline
32. Narkar, V. A., Downes, M., Yu, R. T., Embler, E., Wang, Y. X., Banayo, E., Mihaylova, M. M., Nelson, M. C., Zou, Y., Juguilon, H., Kang, H., Shaw, R. J., and Evans, R. M. (2008) AMPK and PPARδ agonists are exercise mimetics. *Cell* **134,** 405–415 CrossRef Medline
33. Jackson, M. J. (2016) Reactive oxygen species in sarcopenia: should we focus on excess oxidative damage or defective redox signalling? *Mol. Aspects Med.* **50,** 33–40 CrossRef Medline
34. Sullivan-Gunn, M. J., and Lewandowski, P. A. (2013) Elevated hydrogen peroxide and decreased catalase and glutathione peroxidase protection are associated with aging sarcopenia. *BMC Geriatr.* **13,** 104 CrossRef Medline
35. Muller, F. L., Song, W., Jang, Y. C., Liu, Y., Sabia, M., Richardson, A., and Van Remmen, H. (2007) Denervation-induced skeletal muscle atrophy is associated with increased mitochondrial ROS production. *Am. J. Physiol. Regul. Integr. Comp. Physiol.* **293,** R1159–R1168 CrossRef Medline
36. Nakamura, Y. K., and Omaye, S. T. (2009) Conjugated linoleic acid isomers' roles in the regulation of PPAR-γ and NF-κB DNA binding and subsequent expression of antioxidant enzymes in human umbilical vein endothelial cells. *Nutrition* **25,** 800–811 CrossRef Medline
37. Jansen, S., Cashman, K., Thompson, J. G., Pantaleon, M., and Kaye, P. L. (2009) Glucose deprivation, oxidative stress and peroxisome proliferator-activated receptor-α (PPARA) cause peroxisome proliferation in preimplantation mouse embryos. *Reproduction* **138,** 493–505 CrossRef Medline
38. Toyama, T., Nakamura, H., Harano, Y., Yamauchi, N., Morita, A., Kirishima, T., Minami, M., Itoh, Y., and Okanoue, T. (2004) PPARα ligands activate antioxidant enzymes and suppress hepatic fibrosis in rats. *Biochem. Biophys. Res. Commun.* **324,** 697–704 CrossRef Medline
39. Odagiri, H., Kadomatsu, T., Endo, M., Masuda, T., Morioka, M. S., Fukuhara, S., Miyamoto, T., Kobayashi, E., Miyata, K., Aoi, J., Horiguchi, H., Nishimura, N., Terada, K., Yakushiji, T., Manabe, I., *et al.* (2014) The secreted protein ANGPTL2 promotes metastasis of osteosarcoma cells

through integrin $\alpha5\beta1$, p38 MAPK, and matrix metalloproteinases. *Sci. Signal.* **7,** ra7 CrossRef Medline

40. Kadomatsu, T., Endo, M., Miyata, K., and Oike, Y. (2014) Diverse roles of ANGPTL2 in physiology and pathophysiology. *Trends Endocrinol. Metab.* **25,** 245–254 CrossRef Medline
41. Gibson, M. C., and Schultz, E. (1983) Age-related differences in absolute numbers of skeletal muscle satellite cells. *Muscle Nerve* **6,** 574–580 CrossRef Medline
42. Schultz, E., and Lipton, B. H. (1982) Skeletal muscle satellite cells: changes in proliferation potential as a function of age. *Mech. Ageing Dev.* **20,** 377–383 CrossRef Medline
43. Morgan, J. E., and Partridge, T. A. (2003) Muscle satellite cells. *Int. J. Biochem. Cell Biol.* **35,** 1151–1156 CrossRef Medline
44. Pasut, A., Jones, A. E., and Rudnicki, M. A. (2013) Isolation and culture of individual myofibers and their satellite cells from adult skeletal muscle. *J. Vis. Exp.* **2013,** e50074 CrossRef Medline